Micellar and Biochemical Properties of (Hemi)Fluorinated Surfactants Are Controlled by the Size of the Polar Head

Cécile Breyton,[†‡*] Frank Gabel,[§¶‖] Maher Abla,[††] Yves Pierre,[†‡] Florence Lebaupain,[†‡] Grégory Durand,[††] Jean-Luc Popot,[†‡] Christine Ebel,[§¶‖*] and Bernard Pucci[††]

[†]Centre National de la Recherche Scientifique, Institut de Biologie Physico-Chimique, Unite Mixte de Recherche 7099, Paris, France; [‡]Université Paris-7, Paris, France; [§]Commissariat à l'Energie Atomique, IBS, Grenoble, France; [¶]Centre National de la Recherche Scientifique, Unite Mixte de Recherche 5075, Grenoble, France; [‖]Université Joseph Fourier, Grenoble, France; and [††]Laboratoire de Chimie Bioorganique et des Systèmes Moléculaires Vectoriels, Université d'Avignon et des Pays de Vaucluse, Faculté des Sciences, Avignon, France

ABSTRACT Surfactants with fluorinated and hemifluorinated alkyl chains have yielded encouraging results in terms of membrane protein stability; however, the molecules used hitherto have either been chemically heterogeneous or formed heterogeneous micelles. A new series of surfactants whose polar head size is modulated by the presence of one, two, or three glucose moieties has been synthesized. Analytical ultracentrifugation and small-angle neutron scattering show that fluorinated surfactants whose polar head bears a single glucosyl group form very large cylindrical micelles, whereas those with two or three glucose moieties form small, homogeneous, globular micelles. We studied the homogeneity and stability of the complexes formed between membrane proteins and these surfactants by using bacteriorhodopsin and cytochrome b_6f as models. Homogeneous complexes were obtained only with surfactants that form homogeneous micelles. Surfactants bearing one or two glucose moieties were found to be stabilizing, whereas those with three moieties were destabilizing. Fluorinated and hemifluorinated surfactants with a two-glucose polar head thus appear to be very promising molecules for biochemical applications and structural studies. They were successfully used for cell-free synthesis of the ion channel MscL.

INTRODUCTION

Membrane proteins (MPs) need to be isolated from biological membranes for most in vitro studies. This is commonly done with the use of detergents; however, the dissociating effect of detergents can be difficult to control. This often leads to the destabilization and irreversible inactivation of MPs. At least two effects appear to contribute to this phenomenon: 1), detergent micelles can act as a hydrophobic phase into which stabilizing hydrophobic cofactors, lipids, and/or subunits can partition; and 2), the flexible hydrophobic tail of the detergent may interfere with protein-protein interactions that stabilize the native three-dimensional structure (1–3).

In an attempt to overcome these problems, we have been studying the potentialities of fluorinated surfactants (3–6), in which the hydrophobic moiety is fluorinated rather than hydrogenated. They were designed based on the observation that, although alkanes and perfluorinated alkanes are both hydrophobic, they are poorly miscible (7–10). For this reason, surfactants with fluorinated alkyl chains do not partition well into biological membranes (11) and therefore have little cytolytic effect (5,12,13). Their micelles are poor solvents for natural lipids and hydrophobic cofactors, and thus they can be expected to be less delipidating. Furthermore, since their hydrophobic moieties are more bulky and rigid than their hydrogenated counterparts, and they have less affinity for the hydrocarbon-like surface of MP transmembrane segments, they may also be expected to intrude less easily into the protein structure itself. By the same token, however, perfluorinated chains might be expected to be inefficient at preventing MPs from aggregating. To increase the interactions between the hydrophobic domain of MPs and the surfactant, a hydrogenated tip (an ethyl group) can been grafted at the extremity of the fluorocarbon tail, leading to hemifluorinated surfactants (14). In this work, fluorinated and hemifluorinated surfactants are abbreviated as FSs and HFSs, respectively, with (H)FSs referring globally to members of both series. The chemical structure of the tail is specified by subscripts referring to the number of carbons that bear either fluorine or hydrogen atoms (H_2 for an ethyl tip, F_6 for a fluorinated *n*-hexyl core, and H_{10} for a hydrogenated decyl tail; Fig. 1).

In earlier studies, we synthesized and assayed a number of nonionic (H)FSs whose polar head was either a short, polydisperse polymer of Trishydroxymethyl acrylamidomethane (THAM (10); hereafter, (H)F-TAC), a monodisperse polyethyleneglycol group ((H)F-E_8; A. Polidori and B. Pucci, unpublished results), or a chemically defined saccharidic group derived from lactose ((H)F-Lac (15)) or maltose ((H)F-Malt (16); see Fig. S1 in the Supporting Material). Surfactants of the (H)F-TAC series, which are relatively easy to synthesize, were the first (H)FSs to be successfully tested. They proved to be particularly mild toward MPs (5,6) and were successfully tested for applications such as in vitro synthesis of MPs (17) or insertion into preexisting lipid bilayers of (H)FS-solubilized MPs (11,18). The mildness of (H)FSs toward MPs was confirmed with molecules bearing a chemically defined polar head ((H)F-Lac, (H)F-E_8, and (H)F-Malt) (15,16). However, in contrast to

Submitted March 7, 2009, and accepted for publication May 22, 2009.

*Correspondence: Cecile.Breyton@ibpc.fr or christine.ebel@ibs.fr

Editor: Mark Girvin.

0006-3495/09/08/1077/10 $2.00

doi: 10.1016/j.bpj.2009.05.053

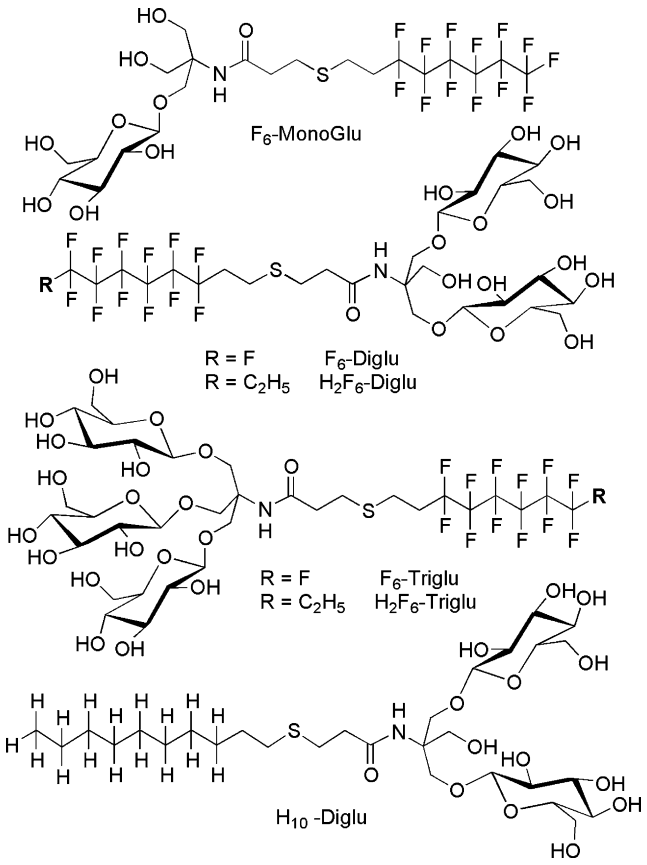

FIGURE 1 Chemical structure of glucose-based hydrogenated, fluorinated, and hemifluorinated surfactants. The structure of the hydrophobic tail, either $C_6F_{13}C_2H_4SC_2H_4$-, $C_2H_5C_6F_{12}C_2H_4SC_2H_4$-, or $C_{10}H_{21}C_2H_4SC_2H_4$-, is denoted by F_6-, H_2F_6-, and H_{10}-, respectively, whereas the abbreviations -Monoglu, -Diglu, and -Triglu refer to the presence in the polar head of one, two, or three β-D-glucose moieties.

(H)F-TACs, which form small micelles, (H)F-Lac and, even more so, (H)F-Malt and (H)F-E_8 were found to form large and polydisperse, probably rod-like assemblies. The complexes they form with MPs are also large and heterogeneous, which is a major drawback for most in vitro studies. These observations led us to design a novel series of (H)FSs with a chemically defined, monodisperse polar head, resulting in the formation of small, globular micelles that would lead to small, monodisperse MP/surfactant complexes while retaining their MP-stabilizing properties.

Some 30 years ago, Tanford (19) and Israelachvili et al. (20) provided general insights into the manner in which the molecular geometry of individual surfactant molecules can control the shape and size of the aggregates they form. The introduction into (H)FSs of a polar head larger than those of (H)F-Lac, (H)F-Malt, or (H)F-E_8, as is the case with (H)F-TAC, must induce an increase of the interfacial curvature of the aggregates, thus favoring the formation of smaller micelles. We tested this hypothesis by designing and synthesizing a new class of (H)FSs whose polar heads are derived from mono-, di-, or triglucosylated THAM, and thus feature similar chemical properties but different bulks (Fig. 1) (21). Surface tension measurements confirmed that grafting one, two, or three glucose moieties, leading respectively to F_6-Monoglu, $(H_2)F_6$-Diglu, and $(H_2)F_6$-Triglu, increased the molecular area of the monomer at the air/water interface. The latter correlated with the nature and size of the aggregates formed in aqueous solutions, as measured by dynamic light scattering (DLS). Whatever the nature of the tail, $(H_2)F_6$-Diglu and $(H_2)F_6$-Triglu surfactants led to the formation of small and well-defined micelles, whereas F_6-Monoglu formed large and heterogeneous aggregates (21).

In this work, we further investigated the type of aggregates formed by these surfactants using analytical ultracentrifugation (AUC) and small-angle neutron scattering (SANS) to characterize their shape, dimensions, aggregation number, etc. We evaluated the potential of these new surfactants in biochemistry using two photosynthetic, colored proteins: bacteriorhodopsin (BR) (22) and the cytochrome b_6f complex from *Chlamydomonas reinhardtii*. Some of these studies were extended to $(H_2)F_6$-Trigal, which is similar to $(H_2)F_6$-Triglu except that it bears galactose rather than glucose moieties (Fig. S1). BR and b_6f were chosen as test proteins because they are relatively fragile when handled in detergent solution (1,23). A molecule of retinal is covalently but loosely bound to BR, whose resulting visible absorption spectrum is a sensitive and convenient reporter of whether it is in its native state. The b_6f is a superdimer that comprises numerous cofactors (24,25). Its activity can be monitored enzymatically (24). Both proteins were purified, with *n*-dodecyl-β-D-maltoside (DDM) for the b_6f, and with *n*-octyl-β-D-thio-glucoside (OTG) for BR, before they were transferred to the (H)FSs to be tested.

MATERIALS AND METHODS

Details are provided in the Supporting Material.

RESULTS

Sedimentation velocity analysis of (H)FS solutions

The sedimentation velocity (SV) experiments combine particle separation and analysis (26). The degree of homogeneity of the preparations can be easily defined, and components of a mixture can be distinguished according to their sedimentation coefficient, *s*. To examine whether the assemblies (H)F-Xglu surfactants (Xglu refers to the whole polar head series) are affected by the H_2O/D_2O content of the solvent, which is varied in SANS contrast matching experiments (see below), comparative measurements were carried out in H_2O and in D_2O buffers, as well as in mixtures thereof.

F_6-Triglu, F_6-Diglu, and H_2F_6-Diglu were found to behave in a similar manner (Fig. 2, *A–E*). Above their respective critical micellar concentration (CMC), each sedimented as a well-defined species—the micelle—with sedimentation coefficients ($s_{20,w}$) of 5.2 ± 0.2 S, 6.2 ± 0.1 S, and 6.4 ± 0.1 S,

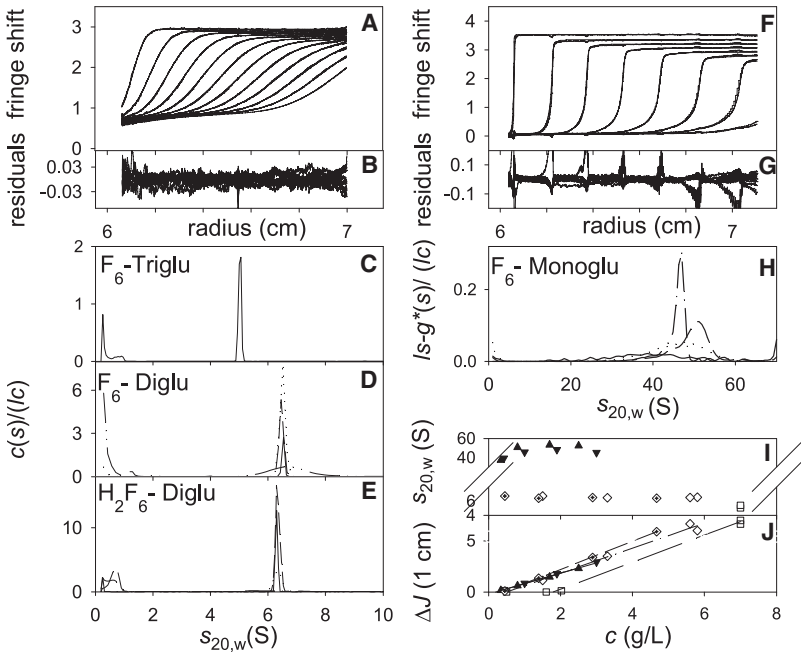

FIGURE 2 SV experiments of (H)F-Xglu surfactants. SV was done at 42,000 rpm, 20°C, using interference optics. Distributions are normalized for the optical path length and surfactant concentration. (*A*) Experimental data (*dots*) collected over 240 min for F_6-Triglu at 6.9 g/L in H_2O, superimposed on modeled profiles (*solid curves*) from the $c(s)$ analysis. (*B*) Corresponding residuals. (*C–E*) $c(s)$ distributions for F_6-Triglu at 6.9 g/L in H_2O (*C*), for F_6-Diglu in the range of 1.5–5.8 g/L in H_2O, D_2O, or 15% D_2O (*D*), and for H_2F_6-Diglu in the range of 0.5–5.0 g/L in H_2O (*E*). In *D* and *E*, the largest concentrations provide the sharpest peaks. (*F*) Superimposition of selected experimental profiles obtained over 30 min for F_6-Monoglu at 3.0 g/L in H_2O and modeled profiles from the ls-$g^*(s)$ analysis. (*G*) Corresponding residuals. (*H*) ls-$g^*(s)$ distributions for F_6-Monoglu at 0.4 (*solid line*), 1.0 (*dotted line*), 1.9 (*dashed line*), and 3.0 (*dashed-dotted line*) g/L. (*I–J*) Concentration dependency for the micelles of F_6-Monoglu in H_2O (▼) and D_2O (▲), F_6-Diglu in H_2O, D_2O, or mixtures thereof (◇), F_6-Triglu in H_2O or D_2O (□), and H_2F_6-Diglu in H_2O (*centered diamond*), of $s_{20,w}$ (*I*) and the normalized fringe shifts (*J*).

respectively. Smaller species with $s_{20,w} < 1$ S were detected in minor amounts, most probably representing the monomer. The behavior in D_2O was similar.

F_6-Monoglu solutions, on the other hand, behaved very differently (Fig. 2, *F–H*). SV experiments were performed in H_2O at concentrations between 0.4 and 3 g/L. Even at the lowest concentration, heterogeneous assemblies were detected, with *s*-values in the 15–65 S range (mean: ~39 S). When the concentration was increased to 1.9 g/L, the mean *s*-value rose to 48 S. For the largest concentration tested, 3 g/L, $s_{20,w}$ decreased to 45 S, most probably due to excluded volume effects. Very similar results were obtained in D_2O (not shown). The mean $s_{20,w}$-values obtained for all (H)F-Xglu molecules are compiled in Fig. 2 *I*. The plot emphasizes how strongly the behavior of F_6-Monoglu differs from that of F_6-Diglu, H_2F_6-Diglu, and F_6-Triglu.

The *s*-value is a function of the particle mass, *M*, partial specific volume, $\bar{v}$ which can be estimated from the chemical composition, and hydrodynamic radius, R_S. The minimum values of *M* that are compatible with experimental *s*-values, i.e., those corresponding to compact, spherical micelles (frictional ratio $f/f_{min} = 1.2$), can be derived using Svedberg's equation. These estimates yielded minimal masses of 35, 44, and 52 kDa for F_6-Triglu, F_6-Diglu, and H_2F_6-Diglu micelles, respectively, and 700 kDa for F_6-Monoglu ones (from the mean *s*-value at 0.4 g/L), corresponding to minimum R_S-values of 2.4, 2.6, 2.8, and 6.5 nm, and minimal aggregation numbers (N_{agg}) of 34, 50, 59, and 1000, respectively. For F_6-Monoglu, the frictional ratio of the very elongated tropomyosin ($f/f_{min} = 3$) is probably more appropriate (see the SANS analysis below). It leads to three to four times larger values of *M*, N_{agg}, and R_S (Table 1). For samples with well-defined micelles, analysis of the boundary spreading of the SV profiles gives access to their translational diffusion coefficient, *D*, which is directly related to R_S. The R_S-values thus derived are 2.4, 3.5, and 3.0 nm for F_6-Triglu, F_6-Diglu, and H_2F_6-Diglu, respectively, which is close to the minimal values estimated above, indicating that the micelles are indeed globular and compact. They are also in reasonable agreement with the estimates previously derived from DLS measurements (21). Combining *D* and *s* provides independent estimates of micellar masses of ~37, ~60, and ~55 kDa for F_6-Triglu, F_6-Diglu, and H_2F_6-Diglu, respectively, which are close to the minimum values calculated above. The estimates of micellar properties are summarized in Table 1.

The SV can also be used to estimate CMCs. SV profiles for F_6-Triglu at 1.6 and 0.5 g/L in D_2O did not allow the detection of the micelles. The $c(s)$ analysis of F_6-Triglu at 2 g/L in H_2O shows a very small contribution of a species at 2.5 S, which may represent micelles in minor amounts or artifacts. The CMC is thus ~2 g/L (1.9 mM) in H_2O and >1.6 g/L (1.5 mM) in D_2O. From the neat linear relationship between the fringe displacement related to micelle sedimentation and the surfactant concentration (Fig. 2 *J*), we estimate CMCs of 0.6 g/L (0.7 mM) for F_6-Diglu in H_2O, D_2O, or mixtures (the data were treated together); 0.4 g/L (0.4 mM) for H_2F_6-Diglu in H_2O; and 0.20 g/L (0.3 mM) for F_6-Monoglu in H_2O and D_2O (the data were treated together; estimated errors: ± 0.1 g/L, or ~ ± 0.1 mM). The plot also provides, from the slope of the regression lines, estimates of the refractive index increments $\partial n/\partial c$, which are reported in Table 1.

In summary, the SV analyses show that F_6-Triglu, F_6-Diglu, and H_2F_6-Diglu form small, well-defined, globular micelles, whereas F_6-Monoglu forms heterogeneous and very large species.

TABLE 1 Micellar and molecular properties of surfactants of the (hemi)fluorinated Xglu series

Compound	F_6-Triglu	F_6-Diglu	F_6-Monoglu	H_2F_6-Diglu
M (kDa)	1041.77	879.63	717.49	889.7
$\bar{v}$ (mL g^{-1})	0.594*	0.585*	0.571*	0.612*; 0.639†
$\partial n/\partial c$ (mL g^{-1})	N. D.	0.083	0.068	0.094
Defined micelles ?				
SANS	yes	yes	no	N. D.
AUC	yes	yes	no	yes
$s_{20,w}$ (S)	5.2 ± 0.2	6.2 ± 0.1	15–65	6.4 ± 0.1
Association state:				
AUC: M (kDa)	≥35‡; 37§	≥44‡;60§	>700‡,¶; ≈2600‖	≥52‡, **; 55§, **
AUC: N_{agg}	≥34‡; 35§	≥50‡; 68§	>1000‡,¶; ≈3600‖	≥59‡, **; 62§, **
SANS: M (kDa)	36	59	≈2300††	
SANS: N_{agg}	34	67	≈3200††	
Dimension (nm)				
AUC: R_S (nm)	≥2.4‡; 2.4 ± 0.3§	≥2.6‡; 3.5 ± 0.1§	≥6.5‡; ≈25‖	≥2.8‡; 3.0 ± 0.2§
SANS: R_g (nm)	1.8 ± 0.1	2.0 ± 0.0	27.5 ± 4.0; R_c = 1.8 ± 0.1	
SANS: Max dim (nm)		5.5‡‡, 5.2§§	100¶¶	
DLS‖‖, ***: R_S (nm)	2.5	2.9	12.6	3.2
DLS‖‖, ***: D (cm^2 s^{-1})	8.6 10^{-7}	7.4 10^{-7}	1.7 10^{-7}	6.7 10^{-7}
Molecular area (nm^2) ***	1.14	0.97 ± 0.02	0.53 ± 0.02	1.04 ± 0.03
CMC (g L^{-1})				
AUC	≈2; ≥1.6†††	0.6 ± 0.1†††	0.20; 0.19 ± 0.1†††	0.4 ± 0.1†††
SANS	N.D; 1.6 ± 0.3†††	0.6; 0.7 ± 0.2†††	N. D.	N.D.
Surface tension***	0.99 ± 0.04	0.20 ± 0.01	0.08 ± 0.01	0.31 ± 0.03
	0.95 ± 0.04 mM	0.23 ± 0.01 mM	0.11 ± 0.01 mM	0.35 ± 0.03 mM

*From chemical formula.
†From density, ± 0.005.
‡Minimum values of M, N_{agg}, and R_S evaluated from s considering f/f_{min} = 1.2, i.e., a globular compact shape.
§From SV analysis in terms of s and D.
¶From $s_{20,w}$ = 39 S at 0.4 g L^{-1}.
‖From s, considering f/f_{min} = 3 (very elongated shape).
**Considering $\bar{v}$ from formula.
††At 3 g L^{-1}.
‡‡From pair distribution in H_2O.
§§From the modeling of the micelle in H_2O/D_2O in terms of two concentric spheres.
¶¶From R_g and R_c.
‖‖At ~4 g L^{-1}; D is at 20°C in H_2O.
***From Abla et al. (21)
†††First and second values are in H_2O and D_2O, respectively; the CMC from AUC of H_2F_6-Diglu is in H_2O, and that of F_6-Diglu is from measurements in H_2O, D_2O, or mixture (see the text).

SANS by F_6-Diglu and F_6-Triglu solutions

SANS provides complementary information about the homogeneity, mass, shape, and structure of the aggregates. The two upper curves of Fig. 3 *A* show neutron scattering by F_6-Diglu and F_6-Triglu solutions in D_2O. Similar scattering curves, but with a lower signal/noise ratio, were obtained in H_2O (Fig. S3). The shape of the scattering curves does not vary (within experimental error) as a function of the concentration of F_6-Diglu and F_6-Triglu in the ranges of 1–10 and 6–10 g/L, respectively (Fig. S2), as expected for compact, globular objects (e.g., micelles; see below). The F_6-Triglu scattering curves in D_2O at concentrations below the CMC (1.7 and 0.5 g/L) display no structural features and do not differ, within experimental error, from those observed with pure buffer (not shown), indicating that the monomer is invisible in the experimental Q-range. Fig. S4 *A* shows selected Guinier plots for F_6-Diglu and F_6-Triglu samples. All F_6-Diglu and F_6-Triglu samples display very neat, linear Guinier plots up to large angles, indicative of the presence of homogeneous, globular particles. The steeper slope of the F_6-Diglu scattering curves indicates that the micelles have a slightly larger radius of gyration, R_g, than the F_6-Triglu ones. The R_g-values (2.0 and 1.8 nm, respectively) are independent of sample concentration (Table S1). From an absolute calibration of $I(0)$, molecular masses of 59 and 36 kDa can be calculated for F_6-Diglu and F_6-Triglu micelles, respectively. These values, which are remarkably close to those obtained by AUC, correspond respectively to 67 and 34 molecules per micelle. Estimates of the CMC can be extracted from the position of the intersection with the abscissa of linear fits of the forward scattering intensities $I(0)$ versus the total concentration of surfactant (Fig. S4 *B*). These values, which again are very close to those obtained by AUC, are reported in Table 1.

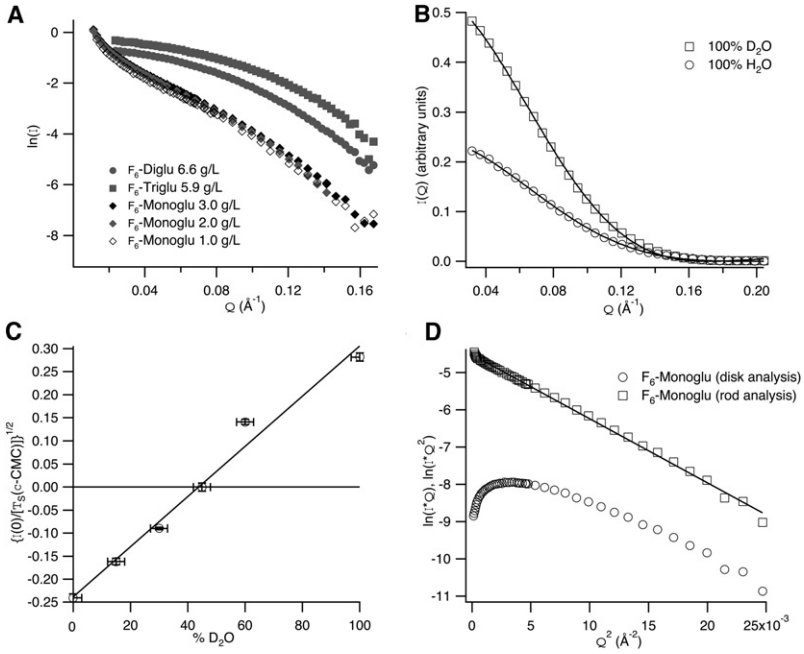

FIGURE 3 SANS analysis of F_6-Xglu solutions. (*A*) Elastic neutron scattering in D_2O by F_6-Monoglu, F_6-Diglu, and F_6-Triglu solutions at the indicated concentrations. Curves for F_6-Monoglu were normalized to the highest concentration. (*B*) Modeling (*line*) of the scattering curves of F_6-Diglu at 3 g/L in H_2O and D_2O in terms of two concentric spheres, with a fixed inner radius $R_2 = 0.9$ nm and free fit outer radius R_1 of 2.6 nm in H_2O and 2.5 nm in D_2O. Relative intensities are respected. (*C*) Plot of normalized forward intensity for F_6-Diglu as a function of the percentage of D_2O in the solvent, yielding a CMP of 44% ± 3% D_2O. (*D*) Plots of $\ln(I(Q) \times Q^2)$ and $\ln(I(Q) \times Q)$ vs. Q^2 for F_6-Monoglu at 3 g/L in D_2O. The first plot is expected to be linear for disk-like objects, whereas the second one is expected to be linear for rod-like ones, which is the case for F_6-Monoglu assemblies. A cross-sectional radius of 1.8 nm was derived from the slope.

Modeling of F_6-Diglu micelles

Neutron scattering by F_6-Diglu solutions was measured in 0, 15, 30, 45, 60, and 100% D_2O (Fig. S3). The analysis of $I(0)$, assuming the CMC to be 0.65 g/L regardless of the D_2O/H_2O ratio (Fig. 3 *C*), gave an experimental contrast match point (CMP) for F_6-Diglu of 44% ± 3% D_2O. This value is close to that of most proteins (~42% D_2O). The less than perfect fit of the experimental data may indicate some degree of polydispersity (27). A theoretical calculation of the CMP from tabulated partial specific volumes and scattering lengths yielded a similar but somewhat different value (52% D_2O). We have no clear explanation for this discrepancy. The scattering at 45% D_2O was indistinguishable from that of water (Fig. S3), and displayed no structural features in the investigated Q-range. F_6-Diglu micelles are completely invisible at this D_2O concentration.

Analysis of the pair-distribution function with the program GNOM (28) (assuming a homogeneous contrast with the solvent) yielded a maximum dimension for F_6-Diglu micelles in H_2O of 5.5 nm. The micelles were modeled as two concentric spheres of radii R_1 (overall radius of micelle) and R_2 (hydrophobic core), with different scattering contrast (CMPs of 87% and 38% D_2O for the hydrophobic core and the outer shell, respectively). The inner radius R_2 was set at 0.9 nm based on an estimate of the length of the F_6-tail, and the outer radius R_1 was adjusted to fit the scattering data (H_2O and D_2O scattering curves at 3 g/L; Fig. 3 *B*). The fits yielded outer radii $R_1 = 2.6$ and 2.5 nm in H_2O and D_2O, respectively, and are in excellent agreement with experimental data up to $Q = 1.4$ nm^{-1} (Fig. S5). These estimates fit very well with the maximum dimension of the micelles estimated from the pair-distribution function.

Scattering curve of F_6-Monoglu superstructures

Fig. 3 *A* also shows scattering curves for F_6-Monoglu in the range of 1–3 g/L. They indicate the presence of larger aggregates compared to those formed by F_6-Triglu and F_6-Diglu. Scattering curves for F_6-Monoglu in H_2O (not shown) look very similar to those in D_2O. The corresponding Guinier plots are not linear (Fig. S6), probably due to polydispersity. For the sample at 3 g/L in D_2O, extrapolation to $I(0)$ of a Guinier plot in the lowest Q-range (0.32–0.58 nm^{-1}) yielded, for the average molecular mass, a lower limit of 2.3 MDa (i.e., ~3200 monomers), and its slope, a lower limit of ~27 ± 4 nm for the average R_g of the particles. The F_6-Monoglu data were analyzed in terms of disk- and rod-like structures (see the Supporting Material). A comparison of the representations $I(Q) \times Q$ vs. Q^2 (rod-like particle) and $I(Q) \times Q^2$ vs. Q^2 (disk-like particle) with the experimental data clearly favored rod-like structures. In this case only was it possible to extract, from a very neat Guinier zone (Fig. 3 *D*), a reasonable cross-sectional radius of gyration (R_C), i.e., 1.8 nm in D_2O and 1.7 nm in H_2O. Assuming that the particles are rod-like, the minimum value of R_g determined above implies a length l of ≥ 0.1 nm.

In summary, SANS analysis confirms that F_6-Diglu and F_6-Triglu form small, well-defined, globular micelles whose shape and size are independent of their concentration and the D_2O content of the solution. F_6-Monoglu forms very large rod-like objects. The molar masses and corresponding aggregation numbers determined by SANS and AUC are similar (Table 1). Neutron scattering by the monomer is negligible even close to the CMC. At their CMP (~45% D_2O), the micelles of F_6-Diglu do not contribute detectably to scattering in the Q-range studied.

Analysis of MP/(H)FS complexes by centrifugation in sucrose gradients

Centrifuging an MP in a sucrose gradient is a convenient means of exchanging the detergent in which the protein was purified for the surfactant to be tested. In the case of colored proteins such as the b_6f or BR, the band is visible. Its position in the gradient is a function of the size, mass, shape, and density of the complexes, whereas the width of the band depends on their homogeneity. Fig. 4 *A* shows the migration of the b_6f in gradients containing 1.5–2 mM of F_6-Triglu, F_6-Diglu, or F_6-Monoglu, which is relatively close to their CMC, or a higher concentration (5 mM), ensuring the presence of a large excess of micelles. For comparison, control experiments were run in DDM at either 0.2 mM, i.e., slightly above the CMC (~0.17 mM), or 5 mM. In 0.2 mM DDM, the b_6f migrates as a monodisperse superdimer (1). In the presence of (H)FSs, it enters much farther into the gradient. This can reflect a higher mass (due to the aggregation of the protein and/or to a higher mass of bound detergent) and/or a higher density of the b_6f/(H)FS complexes as compared to the b_6f/DDM ones. A lower position of the band was also observed in the presence of H_2F_6-Diglu, H_2F_6-Triglu, F_6-Trigal, and H_2F_6-Trigal (not shown), as noted previously with other (H)FSs (6,15,16). We demonstrated previously that, in the presence of HF-Lac (whose $\bar{v}$ is close to that of F_6-Diglu), the b_6f migrates as a dimer (15). We therefore attribute the lower position of the b_6f bands in gradients containing (H)FSs to the higher density of the surfactant bound to the protein, a consequence of the presence of the fluorine atoms (see the low $\bar{v}$-values in Table 1).

In gradients containing 5 mM DDM, a lighter band of the b_6f is present, which results from the partial dissociation of the b_6f into (inactive) monomers (1). Unlike in DDM, no trace of monomerization was observed when the (H)FS concentrations were increased to 5 mM, whether in F_6-Triglu or F_6-Diglu (Fig. 4 *A*) or in H_2F_6-Diglu, H_2F_6-Triglu, F_6-Trigal, or H_2F_6-Trigal (data not shown). A striking result is the broadness of the b_6f band in F_6-Monoglu (Fig. 4 *A*), which suggests polydispersity. This could be due to protein aggregation upon surfactant exchange, e.g., due to a lack of surfactant. However, the band becomes even broader when the surfactant concentration is raised from 1.5 to 5 mM, making this hypothesis unlikely. This behavior is reminiscent of that of the pure surfactant, as seen by AUC and SANS (Figs. 2 *H* and 3 *A*). We thus attribute the polydispersity of the b_6f/F_6-Monoglu complexes to that of the pure surfactant micelles.

Similar results were obtained with BR (Fig. 4 *B*). In OTG or H_{10}-Diglu, BR migrates as a homogeneous band, most likely a monomer (29,30). When BR is transferred to F_6-Triglu, H_2F_6-Triglu, F_6-Diglu, or H_2F_6-Diglu, it migrates deeper than in detergent-containing gradients (Fig. 4 *B*). In 2 mM F_6-Trigal and H_2F_6-Trigal, BR behaves as in F_6-Triglu and H_2F_6-Triglu, respectively (not shown). As for the b_6f, the lower position of the BR band is most likely related to the high density of (H)FSs. Indeed, we previously showed that BR complexed by F-TAC (whose density is close to that of F_6-Diglu) migrates as a monomer. In gradients containing either 1.5 or 5 mM F_6-Monoglu, BR migrated as a broad and diffuse band (Fig. 4 *B*), as did the b_6f. Here

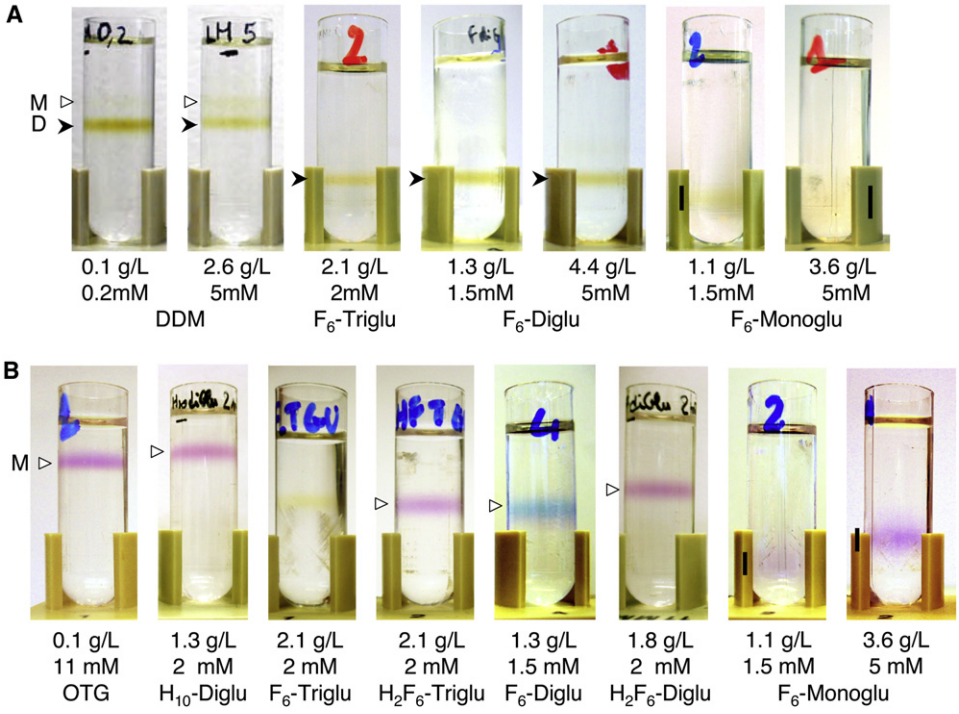

FIGURE 4 Sedimentation analysis of the b_6f (*A*) and BR (*B*) on 10–30% sucrose gradients in the presence of detergents or (hemi)fluorinated surfactants at the indicated concentrations. The gradients were centrifuged 4 h at 200,000 × *g*. D: dimer (*solid arrowhead*); M: monomer (*open arrowhead*). Note that the tubes were not always filled to the same volume, which led to slight variations in the position of the protein band.

again, this behavior is likely related to the polydispersity of the surfactant's micelles. As mentioned above, centrifuging an MP in a sucrose gradient is a convenient means of exchanging surfactants without consuming excessive amounts thereof. We used thin-layer chromatography analysis of a fractionated gradient to ensure that, in the case of BR in OTG, no detergent comigrated with the protein within the limit of detection (<4 mM OTG, i.e., half the CMC). We did not perform a detailed analysis of the complex in terms of lipid composition, but given that the (H)F micelles are a poor solvent for the lipids, it seems highly likely that, as in the case of BR/APol complexes (30), all of the lipids would remain associated to the protein.

Another notable observation is the color of the BR bands (Fig. 4 *B*). Fig. S7 shows the absorption spectra of some of the BR fractions. Whereas in H_{10}-Diglu (Fig. S7 *A*), H_2F_6-Triglu (Fig. S7 *C*), H_2F_6-Trigal (not shown), and H_2F_6-Diglu (Fig. S7 *B*), BR retains its native purple color (λ_{max} = 554–560 nm), the band is yellow in F_6-Triglu (Fig. 4 *B*) and F_6-Trigal (not shown), and blue in F_6-Diglu (Fig. 4 *B* and Fig. S7 *D*). The yellow color (λ_{max} = 380 nm) is due to the presence of free retinal, which is released upon protein denaturation. The blue color (λ_{max} ~ 615 nm), on the other hand, indicates that the cofactor is still bound to the protein by a protonated Schiff base, but its environment has changed. This bathochromic shift appears to be a general feature of monomeric BR in surfactants with perfluorinated tails. The absorption spectrum of the dimeric b_6f, on the other hand, remains unchanged, whether in DDM or (H)FSs. In particular, the absorption maximum of the chlorophyll molecule, which undergoes a bathochromic shift upon monomerization of the complex (1,31), is unaffected after transfer in (H)FSs.

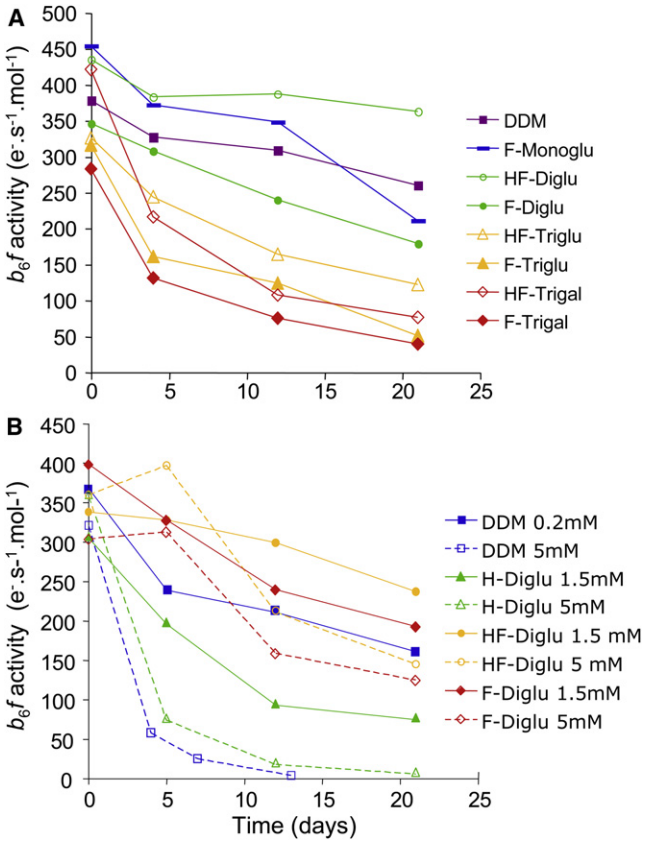

FIGURE 5 Evolution over time of the enzymatic activity of the b_6f upon (*A*) incubation in different surfactants of the Xglu series at low surfactant concentration and (*B*) incubation in low or higher concentrations of either DDM or surfactants of the Diglu series. Samples were collected from the sucrose gradients and kept at 4°C in the dark. Electron transfer activity was as described previously (24).

Biochemical stability of MPs in glucose-based (H)FSs

Effect of the nature of the surfactant head on the stability of MPs

After sucrose gradient centrifugation, protein/surfactant complexes can be collected and further characterized enzymatically and/or spectroscopically. Fig. 5 *A* shows the evolution of the activity of dimeric b_6f upon storage at 4°C in the dark. After transfer to 1.5 mM F_6-Monoglu, F_6-Diglu, or H_2F_6-Diglu, the stability of the b_6f is comparable to that observed in 0.2 mM DDM. In 1.5 or 2 mM F_6-Triglu, H_2F_6-Triglu, F_6-Trigal, or H_2F_6-Trigal, however, the b_6f is less stable. The same pattern is found with BR: when incubated in 1.5 mM H_2F_6-Diglu or F_6-Diglu, the protein is stable over at least 25 days (Fig. S7, *B* and *D*); in 2 mM H_2F_6-Triglu, it is partially denatured after 21 days (Fig. S7 *C*); in 2 mM H_2F_6-Trigal, the retinal is completely released after 5 days (Fig. S7 *C*); and in 2 mM F_6-Triglu (Fig. 4 *B*) or F_6-Trigal (not shown), BR denatures during the centrifugation.

Effect of the surfactant tail

Within the Diglu series, the stability of the b_6f was examined at two surfactant concentrations (Fig. 5 *B*). At 1.5 mM surfactant, b_6f is less stable in H_{10}-Diglu than under control conditions (0.2 mM DDM), whereas its stability is similar in F_6-Diglu and higher in H_2F_6-Diglu. At 5 mM surfactant, i.e., in the presence of a large excess of micelles, the b_6f is rapidly inactivated by hydrogenated surfactants (compare 0.2 and 5 mM DDM or 1.5 and 5 mM H_{10}-Diglu; Fig. 5 *B*), whereas it is almost as stable in 5 mM as in 1.5 mM F_6-Diglu or H_2F_6-Diglu (Fig. 5 *B*). This stability at high F_6-Diglu or H_2F_6-Diglu concentrations is consistent with the absence of a band of the monomeric b_6f in the corresponding sucrose gradients (Fig. 4 *A*). The stabilizing character of (H)FSs as compared to detergents is also obvious in the case of BR, which is partially denatured after 25 days in the presence of 7 mM H_{10}-Diglu (Fig. S7 *A*), whereas it is stable when incubated in the same concentration of H_2F_6-Diglu (Fig. S7 *B*). These observations, which are similar to those previously made with the (H)F-TAC and

(H)F-Lac series (6,15), further confirm the protective effect of a (hemi)fluorinated tail in comparison with a hydrogenated tail.

In F_6-Diglu at low concentration (Fig. S7 *D*), blue BR is biochemically stable after 23 days of incubation (as seen by the absence of free retinal at 380 nm). The UV spectrum of the preparation, however, presents a sloping background due to light diffusion, suggesting the onset of aggregation. At higher F_6-Diglu concentration, a degree of destabilization of BR is noticeable after 23 days, as shown by the lower absorption at 615 nm. The instability of blue BR in FS had already been noted with F-TAC, in which it was only stable for a few hours at high surfactant concentration (F. Lebaupain and C. Breyton, unpublished results).

F_6-Diglu and H_2F_6-Diglu are compatible with cell-free synthesis of MPs

The use of (H)FSs for synthesizing MPs in vitro was previously demonstrated with (H)F-TAC, with a two-transmembrane α-helix, pentameric ion channel, MscL, used as the model. Once purified and inserted into vesicles, MscL behaved as an active channel, suggesting correct folding and oligomerization (17). The innocuousness of the $(H_2)F_6$-Diglu surfactants in a cell-free system was tested using the Roche RTS lysate. Fig. S8 shows that, regardless of the surfactant used, the synthesis level of MscL is similar to that in the absence of surfactant, showing that neither H_{10}-, F_6-, nor H_2F_6-Diglu interfere, at the concentration tested (5 mM), with the transcription/translation machinery. Unlike in the absence of surfactant, MscL is exclusively recovered in the supernatant after centrifugation, indicating that the newly synthesized protein is soluble in the three surfactants.

DISCUSSION

Solution structure of surfactant assemblies

In keeping with DLS measurements (21), AUC and SANS data (this work) indicate that (H)FSs whose polar head bears two or three glucose groups form well-defined micelles. F_6-Triglu micelles comprise ~35 molecules, whereas those of F_6-Diglu or H_2F_6-Diglu ~60. The difference in aggregation numbers must result from the larger size of the Triglu polar head as compared with the Diglu one. Indeed, the same kind of behavior has been reported for detergents with polyoxyethylene polar heads: the aggregation numbers of C_8E_6 and C_8E_4 are ~32 and ~82, respectively, whereas those for $C_{16}E_{21}$, $C_{16}E_{12}$, and $C_{16}E_9$ are ~70, ~150, and ~280 (32). In all three series, the detergents share the same tail (C_8, C_{16}, or F_6), and the aggregation number increases as the size of the polar head decreases. The large difference in aggregation numbers is expected to affect only slightly the Stokes radius, which, for homothetic particles, evolves as $M^{1/3}$. R_S, as a result, should increase by only ~17% for F_6-Diglu as compared with F_6-Triglu. Indeed, experimental estimates of R_S (~3.5 nm) and R_g (~1.9 nm) are essentially the same for the two surfactants, within experimental error, even though the mass of the micelles increases from ~37 to ~60 kDa (Table 1).

The micellar behavior of F_6-Monoglu, whose polar head bears only one glucosyl group, is drastically different. DLS measurements show aggregates with R_S ~13 nm, as compared with ~3 nm for F_6-Tri- and F_6-Diglu (21). AUC shows very heterogeneous samples with an aggregation number that increases dramatically with concentration in the millimolar range. SANS identifies these assemblies as thin rods of 0.1 μm length. As expected for surfactants, their cross-sectional radius of gyration (~1.8 nm) compares very well with the R_g of the globular micelles formed by F_6-Triglu and F_6-Diglu (1.8 and 2.0 nm). The same propensity to form rod-like aggregates was experimentally found, and modeled using molecular dynamics, for F_6-Lac, which bears the same tail and whose polar head has a cross-section similar to that of F_6-Monoglu (Fig. S1) (15).

The CMC values measured by AUC and SANS for (H)FSs are about twice those previously determined by surface tension measurements (21). Irrespective of the technique employed, however, they all show an increase by a factor of 3 $\pm$ 1 for F_6-Diglu as compared to F_6-Monoglu, and for F_6-Triglu as compared to F_6-Diglu. The increase of the CMC is clearly related to the number of glucose groups, i.e., most likely to the rising free-energy cost of packing increasingly conical molecules. For F_6-Triglu, this same constraint causes a drastic drop of the aggregation number.

All measurements give a rather coherent picture of the physical-chemical properties of the (H)F-Xglu series: 1), the larger the polar headgroup, the higher the CMC; and 2), $(H_2)F_6$-Diglu and $(H_2)F_6$-Triglu form well-defined micelles of similar size (F_6-Triglu with a notably smaller aggregation number), whereas F_6-Monoglu assembles into thin, very long and heterogeneous rods. The shape of surfactant aggregates is known to result from a compromise between the repulsion between headgroups and the drive to minimize contacts between apolar chains and water. These opposite constraints can be represented by the ''packing parameter'', P, defined as the ratio between the volume of the tail and the product of the cross-sectional area of the headgroup and the length of the hydrophobic tail. The successive formation of bilayers, cylindrical aggregates (rods), and globular micelles is associated with the value of P decreasing progressively further away from that ($P = 1$) for a regular cylindrical molecule to that ($P < 0.3$) for a conical one (20). In the case of the F_6-Xglu series, the length and volume of the hydrophobic tail remain constant, whereas the area of the headgroup increases with the number of glucose moieties (Table 1). This results in a decrease of P, which is expected to drive the formation of more spherical and compact assemblies, as observed.

Potential of glucose-based (H)FSs for biochemical and structural studies of MPs

Influence of micelle dispersity on the dispersity of MP/surfactant complexes

Ultracentrifugation analyses of the complexes formed by the b_6f and BR with surfactants of the F_6-Xglu series show a clear correlation between the solution behavior of the surfactant alone and the size and homogeneity of protein/surfactant complexes: homogeneous complexes are formed with surfactants that assemble into small, well-defined micelles, whereas F_6-Monoglu, which forms large and heterogeneous rods, leads to polydisperse MP/FS complexes. Although a degree of protein oligomerization cannot be completely ruled out, especially in the case of BR, heterogeneous surfactant binding to the protein is probably the main reason for this polydispersity. A correlation between large and heterogeneous surfactant aggregates and polydisperse MP/surfactant complexes was previously observed with (H)F-Malt (16), (H)F-E_8, and, to a lesser extent, (H)F-Lac (15). For all of these (H)FSs, DLS showed the presence of aggregates with a minimum hydrodynamic radius at 25°C of ~5 nm, which increased with decreasing temperature or increasing concentration (15,16).

Protein stability as a function of polar head size

Both the b_6f and BR are either as stable or much more stable (depending on the surfactant concentration) in solutions of F_6-Monoglu or $(H_2)F_6$-Diglu than they are in the presence of detergents. However, they are much less stable in $(H_2)F_6$-Triglu or -Trigal (Figs. 4 and 5 and Fig. S7). Thus, it is tempting to conclude that the size of the headgroup affects the stability of the protein. Such a correlation was previously noted in a systematic study of the stability of Ca^{2+}-ATPase in different detergents (33). It is likely that the surfactant's molecular shape influences its packing at the surface of the protein hydrophobic transmembrane surface. It has been proposed that the stability of MPs in detergent solutions depends on this surface being efficiently shielded from any contact with water (34). Too large a polar head could work against an efficient coverage, leading to protein inactivation. Alternatively, surfactants whose bulky polar head favors the formation of interfaces with a small radius of curvature, as the small aggregation number of $(H_2)F_6$-Triglu micelles shows, may tend to break open the structure of monomeric MPs, like BR, and to fragment multisubunit MP complexes, like the b_6f, leading to inactivation.

Protein stability as a function of the nature of the tail

In this study we confirm, using the b_6f and BR as models, the protective effect of (hemi)fluorinated chains as compared with hydrogenated ones. On the other hand, the advantages of resorting to hemifluorinated rather than fluorinated surfactants do not appear as striking as suggested by earlier studies with (H)F-TACs (6). Judging from the BR stability data, it seems that long-term storage induces somewhat more aggregation and protein destabilization in F_6-Diglu as compared to H_2F_6-Diglu (Fig. S7 *D*). The important shift of the maximum of absorption BR in BR/F_6-Diglu points to a direct influence of the fluorinated tail on the protein structure. Whether this will hold for other MPs remains to be investigated. Given the difficulty and high cost of synthesizing hemifluorinated surfactants, it seems advisable to first consider fluorinated ones, particularly when large amounts of material are needed and when long-term stability and an excellent monodispersity at low surfactant concentrations are not primordial issues.

This study also shows that F_6-Diglu (at least) is well-suited for structural investigations of MPs by SANS (provided they are available in deuterated or partially deuterated form) since 1), the contribution of F_6-Diglu micelles to the scattering curve can be eliminated by contrast-matching over a very large Q-range; 2), the size and shape of the micelles are invariant over a large concentration range; and 3), monomers are invisible regardless of the contrast.

CONCLUSIONS

On the basis of the study presented here, surfactants composed of a fluorinated or hemifluorinated chain combined with a moderately large hydrophilic head (i.e., the $(H_2)F_6$-Diglu series, with two glucose moieties per polar head) appear very promising for biochemical and structural studies of MPs. Indeed, with the two model MPs investigated here (BR and the b_6f), they form complexes that are both homogeneous and much more stable, at high surfactant concentrations and over extended periods, than those formed with detergents under equivalent conditions. Decreasing the size of the hydrophilic head (in the F_6-Monoglu series) leads to stable but heterogeneous MP/surfactant complexes, whereas increasing it (in the $(H_2)F_6$-Triglu and $(H_2)F_6$-Trigal series) leads to homogeneous but unstable complexes.

Previous studies with the (H)F-TAC series have indicated the great potential of (H)FSs for such applications as transferring MPs from the water phase to preformed lipid membranes (11,18), synthesizing MPs in a cell-free medium (17), and stabilizing fragile, detergent-sensitive MP complexes for biochemical and structural studies (6). The inconvenience of the polymeric nature of the polar head of (H)F-TAC, however, had to be overcome before (H)FSs could become more widely used by membrane biochemists and biophysicists. This long-term goal appears to have been achieved with the validation of $(H_2)F_6$-Diglu surfactants presented here.

SUPPORTING MATERIAL

Materials and methods, references, a table, and eight figures are available at http://www.biophysj.org/biophysj/supplemental/S0006-3495(09)01113-8.

We thank A. Appourchaux (IBS) for performing the density and AUC measurements, F. Zito and E. Billon-Denis (IBPC) for a kind gift of RTS

100HY lysate and MscL plasmid, D. Picot for stimulating discussion, J. Zaccaï for help during the SANS experiments on D22 at ILL (Grenoble, France), and the BAG proposal system for beam time.

This work was supported by the Centre National de la Recherche Scientifique; the Paris-7, Avignon, and Joseph Fourier Universities; the CEA; and by grants from the European Union (STREP LSHG-CT-2005-513770 IMPS, Innovative Tools for Membrane Protein Structural Proteomics) and the French Ministry of Research (ANR-07-PCVI-0010-02).

REFERENCES

1. Breyton, C., C. Tribet, J. Olive, J.-P. Dubacq, and J.-L. Popot. 1997. Dimer to monomer conversion of the cytochrome b_6f complex. Causes and consequences. *J. Biol. Chem.* 272:21892–21900.
2. Garavito, R. M., and S. Ferguson-Miller. 2001. Detergents as tools in membrane biochemistry. *J. Biol. Chem.* 276:32403–32406.
3. Gohon, Y., and J.-L. Popot. 2003. Membrane protein-surfactant complexes. *Curr. Opin. Colloid Interface Sci.* 9:15–22.
4. Pucci, B., J. C. Maurizis, and A. A. Pavia. 1991. Télomères et cotélomères d'intérêt biologique et biomédical IV. Les télomères du Tris(hydroxyméthyl)-acrylamidométhane nouveaux agents amphiphiles non ioniques. *Eur. Polym. J.* 10:1101–1106.
5. Chabaud, E., P. Barthélémy, N. Mora, J.-L. Popot, and B. Pucci. 1998. Stabilization of integral membrane proteins in aqueous solution using fluorinated surfactants. *Biochimie.* 80:515–530.
6. Breyton, C., E. Chabaud, Y. Chaudier, B. Pucci, and J.-L. Popot. 2004. Hemifluorinated surfactants: a non-dissociating environment for handling membrane proteins in aqueous solutions? *FEBS Lett.* 564:312–318.
7. Kissa, E., editor. 1994. Fluorinated Surfactants: Synthesis, Properties, Applications. Dekker, New York.
8. Nakano, T. Y., G. Sugihara, T. Nakashima, and S. C. Yu. 2002. Thermodynamic study of mixed hydrocarbon/fluorocarbon surfactant system by conductometric and fluorimetric techniques. *Langmuir.* 18:8777–8785.
9. Mukerjee, P. 1994. Fluorocarbon-hydrocarbon interactions in micelles and other lipid assemblies, at interfaces, and in solutions. *Colloids Surf. A.* 84:1–10.
10. Barthélémy, P., V. Tomao, J. Selb, Y. Chaudier, and B. Pucci. 2002. Fluorocarbon-hydrocarbon nonionic surfactants mixtures: a study of their miscibility. *Langmuir.* 18:2557–2563.
11. Rodnin, M. V., Y. O. Posokhov, C. Contino-Pepin, J. Brettmann, A. Kyrychenko, et al. 2008. Interactions of fluorinated surfactants with diphtheria toxin T-domain: testing new media for studies of membrane proteins. *Biophys. J.* 94:4348–4357.
12. Maurizis, J. C., M. Azim, M. Rapp, B. Pucci, A. A. Pavia, et al. 1994. Disposition in rats and mice of a new fluorinated biocompatible nonionic telomeric carrier. *Xenobiotica.* 24:535–541.
13. Zarif, L., J. G. Riess, B. Pucci, and A. A. Pavia. 1993. Biocompatibility of alkyl and perfluoroalkyl telomeric surfactants derived from THAM. *Biomater. Artif. Cells Immobilization Biotechnol.* 21:597–608.
14. Barthélémy, P., B. Améduri, E. Chabaud, J.-L. Popot, and B. Pucci. 1999. Synthesis and preliminary assessments of ethyl-terminated perfluoroalkyl nonionic surfactants derived from tris(hydroxymethyl)acrylamidomethane. *Org. Lett.* 1:1689–1692.
15. Lebaupain, F., A. G. Salvay, B. Olivier, G. Durand, A. S. Fabiano, et al. 2006. Lactobionamide surfactants with hydrogenated, perfluorinated or hemifluorinated tails: physical-chemical and biochemical characterization. *Langmuir.* 22:8881–8890.
16. Polidori, A., M. Presset, F. Lebaupain, B. Ameduri, J.-L. Popot, et al. 2006. Fluorinated and hemifluorinated surfactants derived from maltose: synthesis and application to handling membrane proteins in aqueous solution. *Bioorg. Med. Chem. Lett.* 16:5827–5831.
17. Park, K. H., C. Berrier, F. Lebaupain, B. Pucci, J.-L. Popot, et al. 2007. Fluorinated and hemifluorinated surfactants as alternatives to detergents for membrane protein cell-free synthesis. *Biochem. J.* 403:183–187.
18. Palchevskyy, S. S., Y. O. Posokhov, B. Olivier, J.-L. Popot, B. Pucci, et al. 2006. Chaperoning of insertion of membrane proteins into lipid bilayers by hemifluorinated surfactants: application to diphtheria toxin. *Biochemistry.* 45:2629–2635.
19. Tanford, C. 1980. The Hydrophobic Effect: Formation of Micelles and Biological Membranes. Wiley, New York.
20. Israelachvili, J. N., D. J. Mitchell, and B. W. Ninham. 1977. Theory of self-assembly of lipid bilayers and vesicles. *Biochim. Biophys. Acta.* 470:185–201.
21. Abla, M., G. Durand, and B. Pucci. 2008. Glucose-based surfactants with hydrogenated, fluorinated, or hemifluorinated tails: synthesis and comparative physical-chemical characterization. *J. Org. Chem.* 73:8142–8153.
22. Pebay-Peyroula, E., G. Rummel, J. P. Rosenbusch, and E. M. Landau. 1997. X-ray structure of bacteriorhodopsin at 2.5 Å from microcrystals grown in lipidic cubic phases. *Science.* 277:1676–1681.
23. Lopez, F., S. Lobasso, M. Colella, A. Agostiano, and A. Corcelli. 1999. Light-dependent and biochemical properties of two different bands of bacteriorhodopsin isolated on phenyl-sepharose CL-4B. *Photochem. Photobiol.* 69:599–604.
24. Pierre, Y., C. Breyton, D. Kramer, and J.-L. Popot. 1995. Purification and characterization of the cytochrome b6f complex from *Chlamydomonas reinhardtii*. *J. Biol. Chem.* 270:29342–29349.
25. Stroebel, D., Y. Choquet, J.-L. Popot, and D. Picot. 2003. An atypical haem in the cytochrome b(6)f complex. *Nature.* 426:413–418.
26. Schuck, P. 2000. Size-distribution analysis of macromolecules by sedimentation velocity ultracentrifugation and lamm equation modeling. *Biophys. J.* 78:1606–1619.
27. Jacrot, B., and G. Zaccai. 1981. Determination of molecular weight by neutron scattering. *Biopolymers.* 20:2413–2426.
28. Svergun, D. I. 1992. Determination of the regularization parameter in indirect-transform methods using perceptual criteria. *J. Appl. Cryst.* 25:495–503.
29. Dencher, N. A., and M. P. Heyn. 1978. Formation and properties of bacteriorhodopsin monomers in the non-ionic detergents octyl-β-D-glucoside and Triton X-100. *FEBS Lett.* 96:322–326.
30. Gohon, Y., T. Dahmane, R. W. Ruigrok, P. Schuck, D. Charvolin, et al. 2008. Bacteriorhodopsin/amphipol complexes: structural and functional properties. *Biophys. J.* 94:3523–3537.
31. Pierre, Y., C. Breyton, Y. Lemoine, B. Robert, C. Vernotte, et al. 1997. On the presence and role of a molecule of chlorophyll a in the cytochrome b6f complex. *J. Biol. Chem.* 272:21901–21908.
32. le Maire, M., P. Champeil, and J. V. Møller. 2000. Interaction of membrane proteins and lipids with solubilizing detergents. *Biochim. Biophys. Acta.* 1508:86–111.
33. Lund, S., S. Orlowski, B. de Foresta, P. Champeil, M. le Maire, et al. 1989. Detergent structure and associated lipid as determinants in the stabilization of solubilized Ca^{2+}-ATPase from sarcoplasmic reticulum. *J. Biol. Chem.* 264:4907–4915.
34. Rosenbusch, J. P. 2001. Stability of membrane proteins: relevance for the selection of appropriate methods for high-resolution structure determinations. *J. Struct. Biol.* 136:144–157.